Metrol. Meas. Syst., Vol. 30 (2023) No. 4, pp. 755–772
DOI: 10.24425/mms.2023.147962

PAN POLSKA AKADEMIA NAUK

METROLOGY AND MEASUREMENT SYSTEMS
Index 330930, ISSN 0860-8229
www.metrology.wat.edu.pl

M&MS

A HYBRID DENOISING METHOD FOR GYROSCOPES BASED ON MULTIPLE SCREENING

Hailong Rong, Tianlei Jin, Hao Wang, Xiaohui Wu, Ling Zou

Changzhou University, Changzhou 213164, China (✉ *rhle_16@163.com, 3022086502@qq.com, 1275415147@qq.com, wh0122_official@163.com, zouling@cczu.edu.cn*)

Abstract

To reduce the random error of *microelectromechanical system* (MEMS) gyroscope, a hybrid method combining improved *empirical mode decomposition* (EMD) and *least squares algorithm* (LS) is proposed. Firstly, based on the multiple screening mechanism, *intrinsic mode functions* (IMFs) from the first decomposition are divided into noise IMFs, strong noise mixed IMFs, weak noise mixed IMFs and signal IMFs. Secondly, according to their characteristics, they are processed again. IMFs from the second decomposition are divided into noise IMFs and signal IMFs. Finally, useful signal is gathered to obtain the final denoising signal. Compared with some other denoising methods proposed in recent years, the experimental results show that the proposed method has obvious advantages in suppressing random error, greatly improving the signal quality and improving the accuracy of inertial navigation.

Keywords: micro electromechanical system, multiple screening mechanism, empirical mode decomposition.

1. Introduction

Microelectromechanical systems (MEMS) have become the basic components of civil navigation because of their low-cost performance, small size and weight, and strong adaptability [1]. Among these ways for improving navigation accuracy, the most effective one is to improve accuracy of MEMS gyroscopes [2]. Improving navigation accuracy through gyroscope noise reduction is a must for civil navigation.

In recent years, scholars from different countries have conducted a large number of in-depth studies on the problem of suppressing random error in gyroscopes, and numerous effective methods have been developed. Among them, the most commonly used methods can be divided into the following three categories: modelling compensation methods, *wavelet threshold denoising* (WTD) methods, and *empirical mode decomposition* (EMD) methods.

Article history: received May 24, 2023; revised August 31, 2023; accepted September 13, 2023; available online November 22, 2023.

The modelling compensation method can reduce the influence of random noise after establishing an error model for it, and then the Kalman filter will compensate the signal. However, in view of the non-stationary, weakly linear and slow time varying characteristic of random error, the accuracy of the error model will affect the compensation effect of the Kalman filter [3]. In 2018, following the mechanism of gyroscope random noise, Cai proposed a direct modelling method and combined it with the Kalman filter to realize the processing of noise [4]. In 2022, Javad Abbasi proposed a method for denoising of long-term MEMS-based gyro error. In this approach, an *auto-regressive* (AR) model for the *long-term error* (LTE) is developed which is used as the process part of a Kalman filter [5]. These methods solve the problem of model accuracy to varying degrees.

Wavelet threshold denoising sets a reasonable threshold to filter out the wavelet coefficient, and retains the large wavelet coefficient, so as to achieve the suppression of the noise signal [6]. The key to this approach is the setting of thresholds. In 2017, Sun proposed a method for MEMS gyroscopes to denoise. His approach combined the sparse decomposition with lifting wavelet transforms [8]. An integrated method for wavelet denoising and time series analysis is proposed by Yingjie Hu in 2018. First, wavelet denoising is employed to dispose of the high frequency noise and then time series analysis combined with a Sage-Husa adaptive Kalman filter is utilized to eliminate the low frequency noise [9]. However, due to the lack of good adaptability of wavelet threshold denoising, the difficulty lies in the selection of the wavelet basis and determination of the threshold function.

Empirical mode decomposition (EMD) is a new adaptive method to deal with nonlinear and non-stationary signals [10]. It does not require any prior knowledge of the signal, nor does it require the establishment of error models. However, its disadvantage is that the mode aliasing phenomenon often occurs [11]. In order to solve this problem, some improved EMD methods are emerging. In 2021, Lang Xu proposed a denoising method based on the *sparrow search algorithm* (SSA) and *variational mode decomposition* (VMD). In order to efficiently extract useful IMFs, they calculated the *mean Mahalanobis distance* (MMD) of the *Fast Fourier Transform* (FFT) function between each IMF and the *residual term* (REST) [12]. In 2022, Li Jian proposed a method for denoising gyroscopes, which used complete *Ensemble EMD with Adaptive Noise* (CEEMDAN) as the Core part, combined with a backpropagation neural network and Kalman filtering [13].

In order to suppress the random noise in gyroscopes, a hybrid method combining EMD and LS is proposed in this paper. In this method, we propose a novel multiple screening mechanism combining the Pearson coefficient, the entropy weight method and Shannon entropy to deal with the mode aliasing phenomenon. IMFs from the first EMD decomposition are divided into four categories: noise IMFs, strong noise mixed IMFs, weak noise mixed IMFs and signal IMFs. Then, according to their different characteristics, the least square algorithm is used to gather useful signal in the strong noise mixed IMFs. The weak noise mixed IMFs are decomposed by EMD again, and IMFs are divided into noise IMFs and signal IMFs by Shannon entropy. Finally, all useful signal is gathered and the final result is obtained. In general, what is unique in this paper is that we not only solve the difficulty of distinguishing IMFs, but also refine the denoising process, making the denoising more effective.

The rest of this paper is organized as follows. Section 2 introduces the mathematical model of the mixed method. Section 3 describes the unique multiple screening mechanism in this paper. Section 4 gives the concrete steps and flow chart of the scheme, and Section 5 shows experiments conducted to verify the method in this paper, which is divided into static experiments and dynamic experiments. Finally, conclusions are drawn in Section 6.

Metrol. Meas. Syst., Vol. 30 (2023), No. 4, pp. 755–772
DOI: 10.24425/mms.2023.147962

2. Mathematical model introduction

2.1. Mathematical model of EMD

In the process of decomposition, the EMD algorithm does not need to set the basis function in advance. It can decompose non-stationary nonlinear signal according to the time characteristic of the signal to obtain several IMFs and a *residual term* (REST) in different time scales [14]. The detailed decomposition process is referred to the literature [15], and a specific flow chart for the EMD algorithm is given here, as shown in Fig. 1.

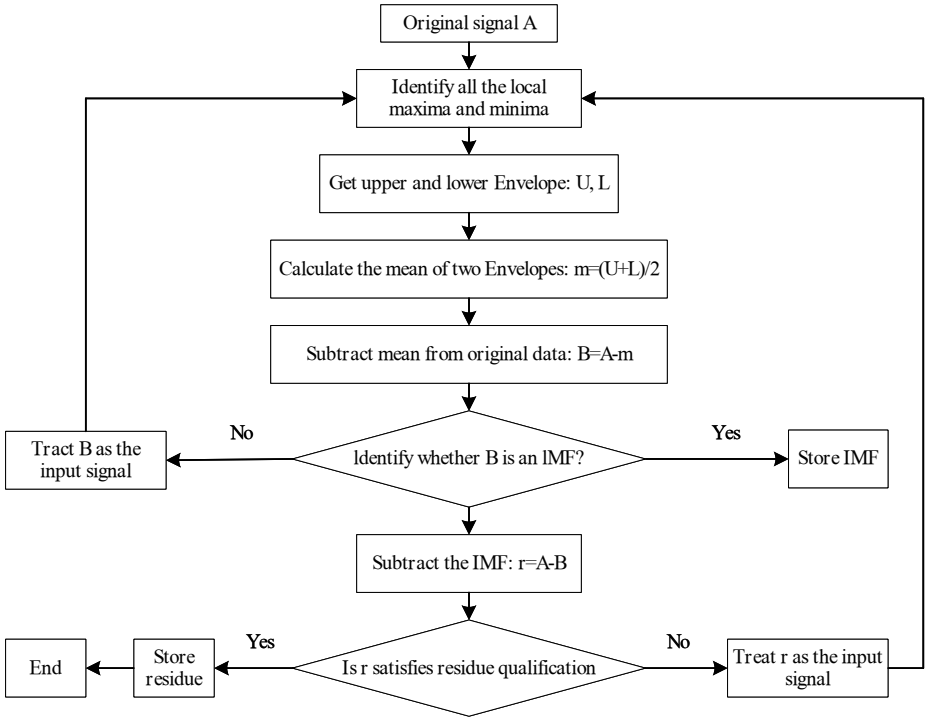

Fig. 1. Detailed procedure of empirical mode decomposition.

The EMD algorithm is used to decompose the signal to obtain the IMFs. These IMFs must satisfy two conditions:

1. The function in the whole-time range, the number of local extreme points and zero crossing points must be equal, or at most one difference;
2. At any point in time, the envelope of the local maximum (upper envelope U) and the envelope of the local minimum (lower envelope L) must be zero on average.

After the decomposition, the original signal is decomposed into IMFs and a residue. Consequently, the signal can be reconstructed in the following form:

$$A = \sum_{i=1}^{L} B_i + r, \tag{1}$$

where, A is the original signal, B_i is an IMF, r is the residue, L is the number of IMFs.

2.2. Least squares algorithm

The LS algorithm is a mathematical optimization technique which looks for the best function match of the data by minimizing the sum of the squares of the errors. The least square method can be used to obtain the unknown data easily and minimize the sum of squares of errors between the obtained data and the actual data [16].

Least square method can also be used for curve fitting.

The core formula of least square fitting curve used in this paper is as follows:

$$F = \frac{1}{2}\sum_{j=1}^{N}(a_j - o_j)^2, \tag{2}$$

where, a_j is the signal generated by the least squares algorithm, o_j is an ideal signal, F is the square of the error, and N is the data length.

In (2), when the value of F reaches the minimum, the fitted signal is closest to the ideal signal. At this point, the fitted signal is the signal we want to obtain.

Due to the limitation of the length, this paper only gives a brief introduction, and the detailed implementation process of the algorithm is referred to in the literature [17].

3. Multiple screening mechanism

Due to the mode aliasing phenomenon of EMD, it is hard to distinguish IMFs that contain useful signal in all IMFs. In view of this difficulty, a multiple screening mechanism is proposed in this paper. This mechanism is composed of the Pearson coefficient, the entropy weight method and Shannon entropy. Their details are as follows:

3.1. Pearson coefficient

The *Pearson correlation coefficient* (PCC) [18] is used in this paper to reflect the degree of correlation between the gyroscope output and IMFs, and its definition is as follows:

$$\mathrm{PCC}_i = \frac{\sum_{j=1}^{N}\left(A_j - \overline{A}\right)\left(B_{ij} - \overline{B}_i\right)}{\sqrt{\left[\sum_{j=1}^{N}\left(A_j - \overline{A}\right)^2\right]\left[\sum_{j=1}^{N}\left(B_{ij} - \overline{B}_i\right)^2\right]}}, \quad i = 1, \ldots, L, \tag{3}$$

where, A_j represents an element in A; $\overline{A}$ is the average of elements in A; B_{ij} represents an element in B_i; $\overline{B}_i$ is the average of elements in B_i; The value range of PCC is [–1, 1], The value of PCC indicates the degree of correlation. The general evaluation criteria for PCC are shown in Table 1.

Since IMFs are distributed from high frequency to low frequency successively, according to the correlation degree criterion of the Pearson coefficient, we can obtain noise IMFs and strong noise mixed IMFs, whereas the main components of noise IMFs are high frequency noise, and strong noise mixed IMFs only contain a little useful information.

Table 1. General evaluation criteria for PCC values.

PCC	Correlation degree
0.00–0.19	Weakest correlation
0.20–0.39	Weak correlation
0.40–0.69	Moderate correlation
0.70–0.89	Strong correlation
0.90–1.00	Strongest correlation

3.2. Entropy weight method

The entropy weight method is an objective weighting method. In the specific application process, according to dispersion of each index data, the entropy weight is calculated by information entropy. Then, the entropy weight is modified to a certain extent based on each index data, so as to obtain a relatively objective index weight [19].

In this paper, the entropy weight method is used to calculate the weight of each IMF. Depending on the weight, we can get IMFs that contain a useful signal. Its mathematical model is as follows:

Data normalization:

$$z_{ij} = \frac{B_{ij} - \min\{B_{1j}, \ldots, B_{Lj}\}}{\max\{B_{1j}, \ldots, B_{Lj}\} - \min\{B_{1j}, \ldots, B_{Lj}\}}, \quad i = 1, 2, 3 \ldots L; \quad j = 1, 2, 3 \ldots N, \tag{4}$$

where, z_{ij} is element after normalization.

Calculate the proportion p_{ij} of each element in the IMF:

$$p_{ij} = \frac{z_{ij}}{\sum_{j=1}^{N} z_{ij}}, \quad i = 1, \ldots, L. \tag{5}$$

Calculate the entropy value e_i of each IMF:

$$e_i = -\frac{1}{\ln L} \sum_{j=1}^{N} p_{ij} \mathrm{In}(p_{ij}), \quad i = 1, \ldots, L. \tag{6}$$

Calculate the redundancy d_i of information entropy (difference):

$$d_i = 1 - e_i, \quad i = 1, \ldots, L. \tag{7}$$

Calculate the weight w_i of redundancy of each information entropy:

$$w_i = \frac{d_i}{\sum_{i=1}^{L} d_i}, \quad i = 1, \ldots, L. \tag{8}$$

Using the entropy weight method, we calculate the weight of each IMF. On the basis of the Pearson coefficient analysis, weak noise mixed IMFs and signal IMFs can be obtained. At this point, IMFs are divided into four categories: noise IMFs, strong noise mixed IMFs, weak noise mixed IMFs and signal IMFs. Then we can choose appropriate approach to handle different categories of IMFs based on their characteristics.

3.3. Shannon entropy

Shannon entropy [20] is a classical method that measures the uncertainty of information. The higher the Shannon entropy of a sample, the more information the sample contains.

In this paper, Shannon entropy is used to calculate useful information contained in IMFs, so as to measure relative importance between IMFs. Its mathematical model is as follows:

$$H(i) = -\sum_{j=1}^{N} \left(\frac{B_{ij}}{A_j}\right) \log\left(\frac{B_{ij}}{A_j}\right), \quad i = 1, \ldots, L, \tag{9}$$

where, $H(i)$ is the Shannon entropy of an IMF.

In order to facilitate observation, on the basis of existing theories, we calculate the sum of IMF entropy, and obtain the percentage of each IMF's Shannon entropy in the sum. The formula is as follows:

$$S(i) = \frac{H(i)}{\sum_{i=1}^{L} H(i)}, \quad i = 1, \ldots, L, \tag{10}$$

where, $S(i)$ represents the proportion of an entropy in the sum of all entropies.

Shannon entropy is used to distinguish IMFs in the second EMD decomposition. Due to the small number of IMFs obtained in the second decomposition, it is not suitable to divide them into four categories with the previous screening method. Here, we use Shannon entropy to divide them into two categories: noise IMFs and signal IMFs.

4. Specific steps of the proposed method

4.1. Steps of our experiment

In order to make experiment clear and reasonable, our experiment is in this paper divided into six parts, and their specific activities are as follows:

Step 1: The output signal of the gyroscope is decomposed into intrinsic mode function terms and the residual term by EMD;

Step 2: According to (3), we calculate the PCC of each IMF. Then, referring to Table 1, we obtain noise IMFs and strong noise mixed IMFs.

Step 3: First, according to (4)–(8), we use the entropy weight method to calculate the weight of each IMF. Then, on the basis of Step 2, we combine the weight and PCC to obtain weak noise mixed IMFs and signal IMFs.

Step 4: Based on characteristics of strong noise mixed IMFs, the least square algorithm is used to gather the signal in strong noise mixed IMFs. Referring to (2), when F is minimum, the useful signal is obtained to the maximum extent.

Step 5: For weak noise mixed IMFs, we adopt EMD decomposition for secondary processing. Then, according to (9) and (10), we use Shannon entropy to classify IMFs. The signal IMFs are retained and the noise IMFs are removed.

Step 6: All useful signals obtained in the previous steps are gathered to obtain the final result.

4.2. Flow chart of the proposed method

In order to make the context of the article clear, we provide a flow chart of the method described in this paper. It is shown in Fig. 2.

Metrol. Meas. Syst., Vol. 30 (2023), No. 4, pp. 755–772
DOI: 10.24425/mms.2023.147962

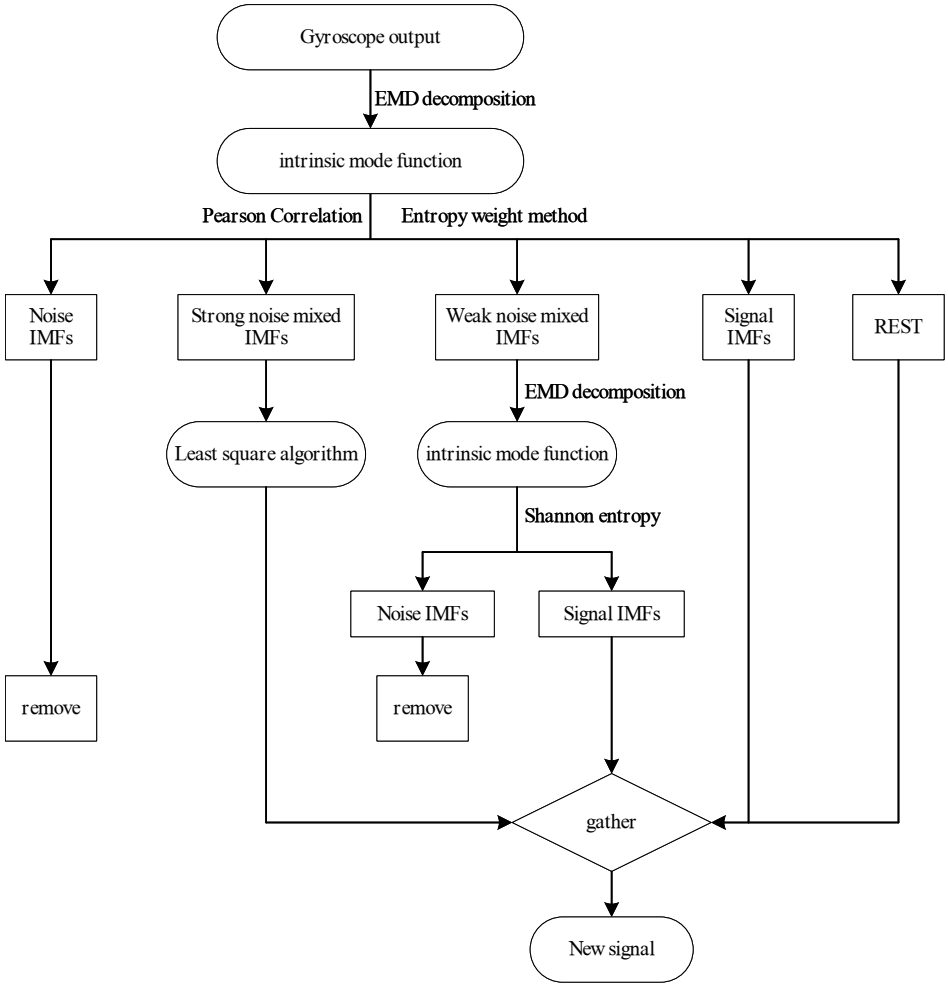

Fig. 2. EMD-Pearson-information entropy flow chart.

As shown in Fig. 2, the unique multiple screening mechanism divides IMFs from the first EMD decomposition into four categories: noise IMFs, strong noise mixed IMFs, weak noise mixed IMFs and signal IMFs. Then IMFs from the second EMD decomposition are divided into noise IMFs and signal IMFs. The difficulty in distinguishing IMFs is addressed and the denoising process is refined.

5. Experimental verification

5.1. Main technical parameters of the inertial measurement unit

The *inertial measurement unit* (IMU) used in this experiment is PA-IMU488B, and its parameters are shown in Table 2.

Table 2. IMU parameters.

Parameters		PA-IMU488B	Unit
Gyroscope	Measuring range	±450	deg/s
	Zero bias stability	2	deg/h
	Random walk	0.1	deg/$\sqrt{h}$
	Zero bias repeatability (−40° ~ +85°C)	0.1	deg/s
	Scale factor repeatability (−40° ~ +85°C)	0.2	%
	Scale factor is nonlinear	0.1	%FS
	Bandwidth	400	Hz
Accelerometer	Measuring range	±6	g
	Zero bias stability	0.1	mg
	Random walk	0.02	m/s/$\sqrt{h}$
	Zero bias repeatability (−40° ~ +85°C)	±5	mg
	Scale factor repeatability (−40° ~ +85°C)	0.5	%
	Scale factor is nonlinear	0.1 FS = 6 g	%FS
	Bandwidth	200	Hz 3dB

5.2. Static experiment

In the static experiment, the MEMS measurement unit was placed on the constant temperature rotary table, and the x-axis of the MEMS gyroscope was taken as the test object to obtain 200,000 data. Because of the instability, the beginning and the ending output data sampled at the early stage and the last stage of the experiment, respectively, were discarded, and as a result, a total of 100,000 data recorded between the 50001th and the 150,000th sampling instants was reserved for later use. The original output of the gyroscope is shown in Fig. 3.

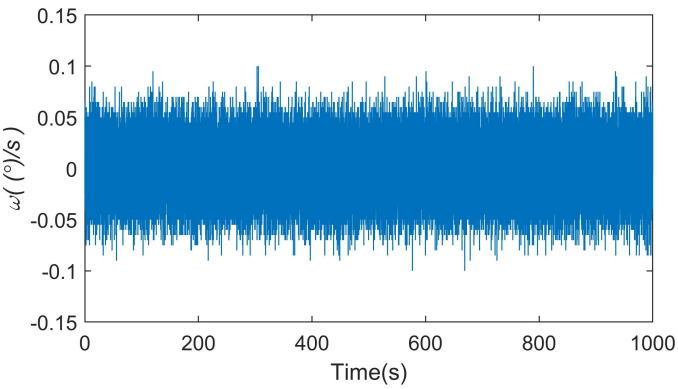

Fig. 3. Original signal from the gyroscope.

5.2.1. EMD decomposition

Following the flow shown in Fig. 1, we use EMD to decompose the raw signal. It can be divided into the following steps:

1. Local maxima and minima are identified to obtain the upper envelope U and lower envelope L, and then calculate the mean of U and L.
2. The mean in Step 1 is subtracted from the original signal. If the result meets the IMF conditions, it is exported as IMF. If not, the steps above are repeated.
3. The IMF is separated from the original signal and Step 1 and 2 are repeated until the residue satisfies the residue qualification. Now, the original signal can be represented by (1).

After EMD decomposition of the original signal above, as shown in Fig. 4, 17 IMFs and a residue are obtained.

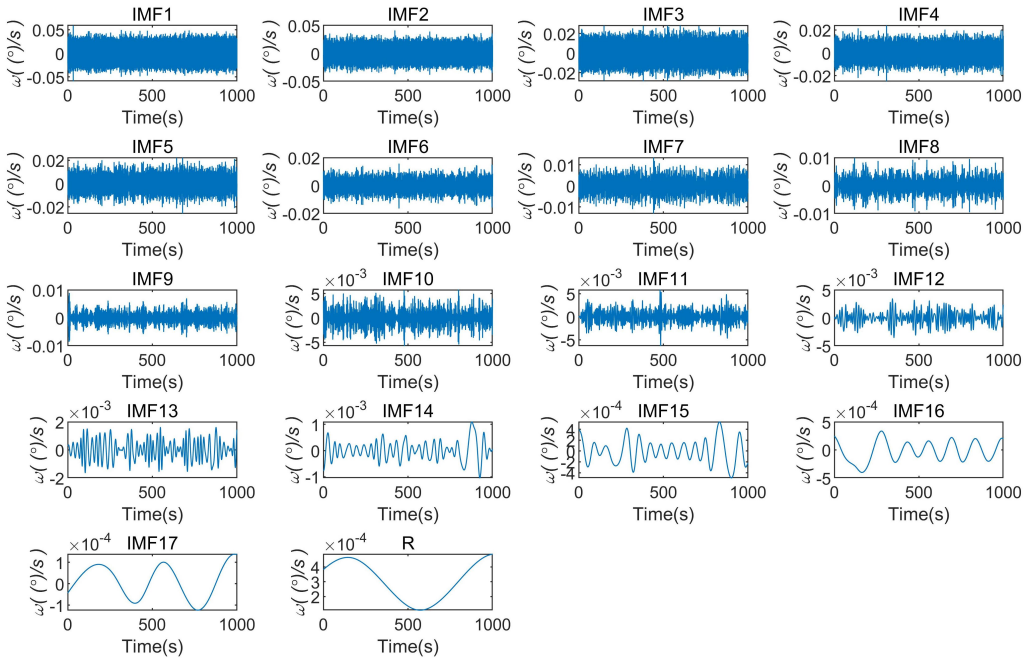

Fig. 4. IMF components and remainder of the original signal.

5.2.2. Pearson correlation coefficient analysis

The Pearson coefficient was used to analyze each IMF. According to (3), we combined the signal data obtained from the experiment to calculate the PCC of each IMF, as shown in Fig. 5. We found that IMF1 had the largest PCC, about 0.7. With the increase of the IMF grade, PCC gradually becomes smaller. According to the evaluation criteria in Table 1, the PCC of IMFs after IMF5 (excluding IMF5) is always within the range [0.00-0.19], with the weakest correlation. Therefore, we consider the first five IMFs to be noise-dominated IMFs. In addition, since the PCC of IMF3, IMF4 and IMF5 are in the range [0.20–0.39], we believe that they are strong noise mixed IMFs, while IMF1 and IMF2 are noise IMFs, which can be removed.

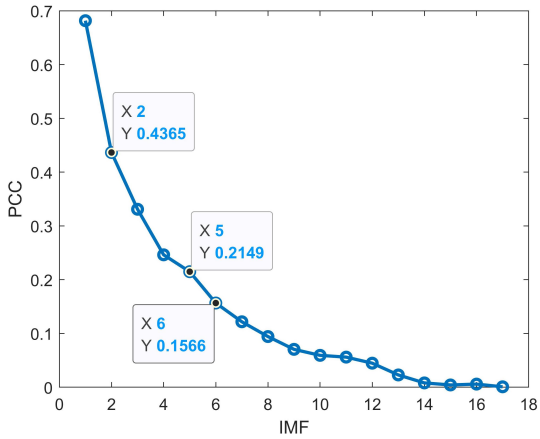

Fig. 5. Pearson correlation coefficient.

5.2.3. Entropy weight analysis

According to (4)–(8), we use the entropy weight method to calculate the weight of each IMF, as shown in Fig. 6. To make it easier to distinguish different IMFs, we propose a method to determine the scope by the mean value in this paper. The sum of weights is 1, and we calculate that the average weight of these IMFs is 0.056. In this paper, we take IMFs that exceed the average, so IMF13 and IMF15-IMF18 are considered signal IMFs. Combined with the Pearson coefficient analysis results above, IMF 14 and IMF6–IMF12 are considered to be weak noise mixed IMFs.

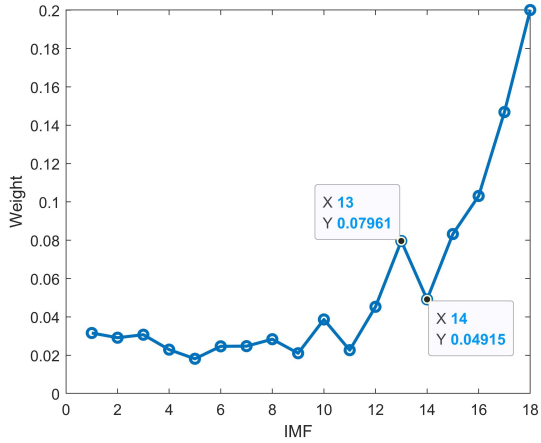

Fig. 6. Entropy weight method.

5.2.4. Mixed IMF reprocessing

After IMFs from the original signal are classified, we gather mixed IMFs again for further processing, as shown in Fig. 7. Among them, the signal in the figure above are strong noise mixed IMFs, which is composed of IMF3, IMF4 and IMF5. The signal below are weak noise mixed IMFs, composed of IMF6–IMF12 and IMF14.

Metrol. Meas. Syst., Vol. 30 (2023), No. 4, pp. 755–772
DOI: 10.24425/mms.2023.147962

At this time, following the results of the Pearson coefficient analysis, it can be concluded that strong noise mixed IMFs (upper part of Fig. 7) are mainly composed of high-frequency noise and contain little useful signals. Therefore, we use the least squares to deal with it. Specifically, we first set o_j to 0, since we are now dealing with static data, then we let F reach its minimum. The critical value of a_j that makes F minimal is just what we require.

Weak noise mixed IMFs (lower part of Fig. 7) contain less noise, so they are not suitable to be directly processed by the least square algorithm, because it is easy to lose useful signals. In this paper, the EMD decomposition is performed again. Fig. 8 is the decomposed IMFs image.

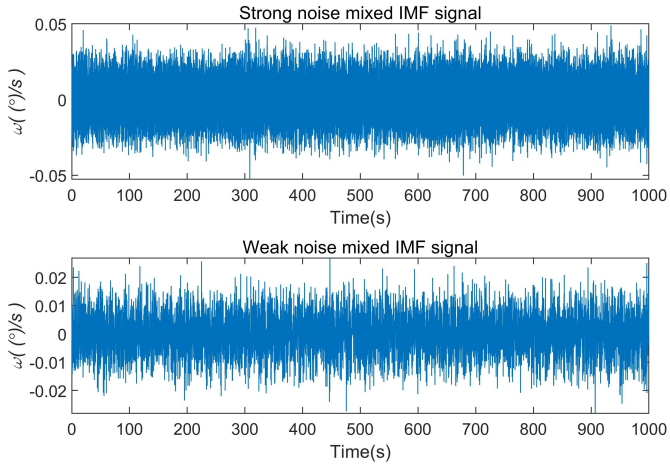

Fig. 7. Signals gathered again by mixed IMFs.

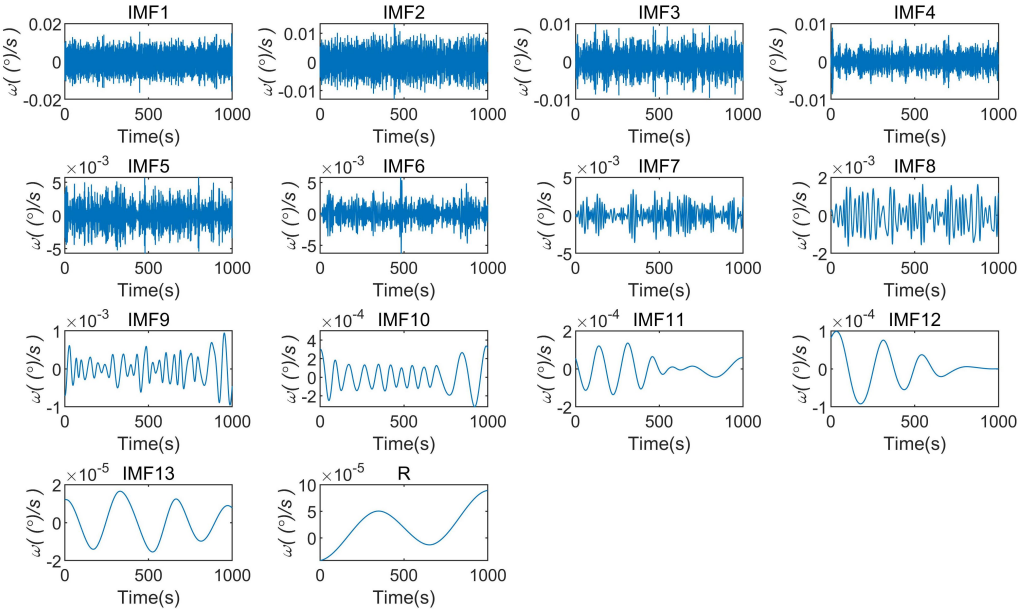

Fig. 8. IMF and R from the quadratic decomposition.

As the characteristics of these IMFs differ, this paper uses improved Shannon entropy to classify IMFs. According to (9) and (10), we calculate the Shannon entropy of each IMF and its proportion in all IMFs, as shown in Figure 9. We calculate that the average Shannon entropy weight for each IMF is 0.077, and like the entropy weight method, we take components that exceed the average. Therefore, IMF7-IMF13 are taken as signal IMFs in this paper, and IMF1-IMF6 are removed.

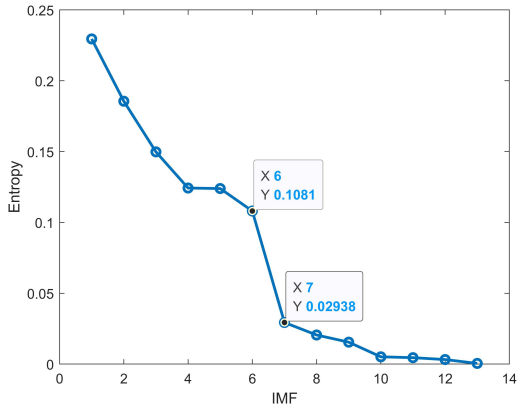

Fig. 9. Information entropy.

5.2.5. Comparison of experimental results

In order to verify the performance of the denoising method presented in this paper, five denoising methods proposed in recent years are compared. Here is a brief description of each method:

Scheme 1 [5]: Low frequency noise is modeled autoregressively, and a Kalman filter compensates the signal.

Scheme 2 [3]: *Empirical mode decomposition* (EMD) decomposes the original signal; Improved mean square error and a probability density function are used as IMF screening criteria.

Scheme 3 [12]: *Variational modal decomposition* (VMD) decomposes the original signal, and VMD parameters are optimized by the sparrow search algorithm.

Scheme 4 [7]: *Complete ensemble empirical mode decomposition* (CEEMDAN) decomposes the original signal, and the *lifting wavelet transform* (LWT) performs the secondary processing.

Scheme 5 [6]: *Empirical Mode Decomposition* (EMD) decomposes the original signal and *modified recursive least square* (MRLS) reconstructs the useful signal.

The result of the comparative experiment is shown in Fig. 10.

In order to verify the reliability of the experimental results, we calculate the *variance* (VAR) and *root mean square error* (RMSE) of the signal after it was denoised with each method. Then, the VAR and RMSE of each method are compared with those of the original signal, as shown in the Table 3.

The calculation results show that, compared with the original gyroscope output signal, the variance of the proposed method is reduced to 0.15% and the root mean square error is reduced to 3.5%, indicating that the proposed method can achieve higher accuracy in static environment compared with other methods.

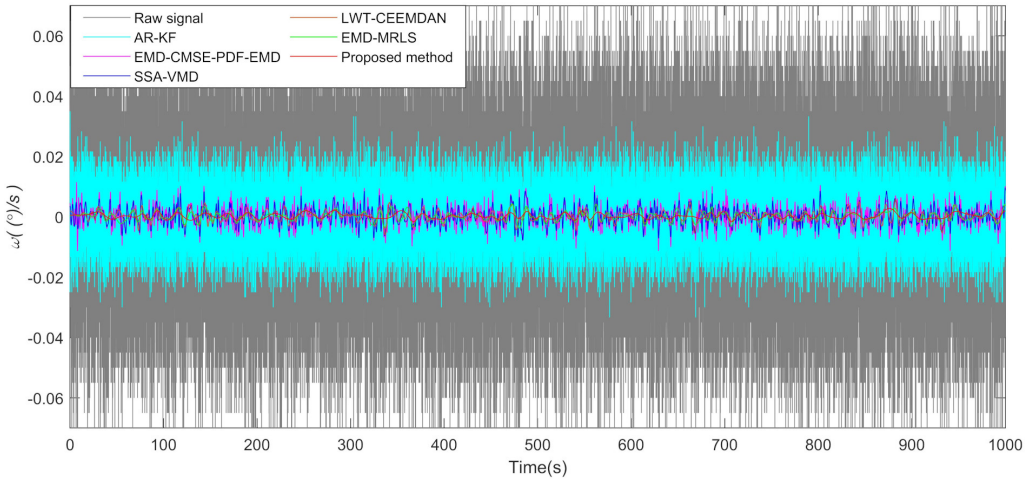

Fig. 10. Comparison of denoising results of the static experiment.

Table 3. Variance and root mean square error of the denoising results.

	Raw signal	**Scheme 1**	**Scheme 2**	**Scheme 3**	**Scheme 4**	**Scheme 5**	**Proposed method**
VAR	5.22e–04	5.81e–05	1.07e–05	7.12e-06	2.90e–06	1.98e–06	6.97e–07
Comparison (VAR)		11%	2%	1.4%	0.6%	0.3%	0.15%
RMSE	0.0228	0.0076	0.0032	0.0026	0.0017	0.0014	0.0008
Comparison (RMSE)		33%	14%	11.4%	7.5%	6.1%	3.5%

5.3. Dynamic experiment

In this paper, the dynamic data is a set of inertial navigation flight data from an unmanned aerial vehicle with the flight speed 100 m/s, the distance about 25 km, the acquisition time 1000 s, the frequency 200 Hz, and the first 200 s are stationary. According to actual flight data, the smooth trajectory parameters are generated by combining the partial feedback principle of the Kalman filter and the three-spline interpolation method. The detailed content of this method can be found in reference [21].

The denoising process of dynamic data is basically the same as that of static data. We still perform the denoising process of dynamic data according to the six steps mentioned above to obtain the final signal. The final experimental results are shown in Fig. 11.

As shown in the figure, compared with other methods, the proposed method has less noise and more accurate angular velocity. This shows that the proposed method has certain advantages in the case of dynamic data.

In order to verify the reliability of the proposed method in a practical application, we respectively used the same method to denoise the accelerometer signal. The denoising method is the same as the noise reduction method for gyroscopes. Then, we combined the denoised gyroscope signal with the accelerometer signal to calculate the triaxial attitude angle of IMU. The attitude calculation method adopted in this paper is the gradient descent method. For detailed steps, refer to the literature [22]. The results of the attitude approach are shown in Fig. 12.

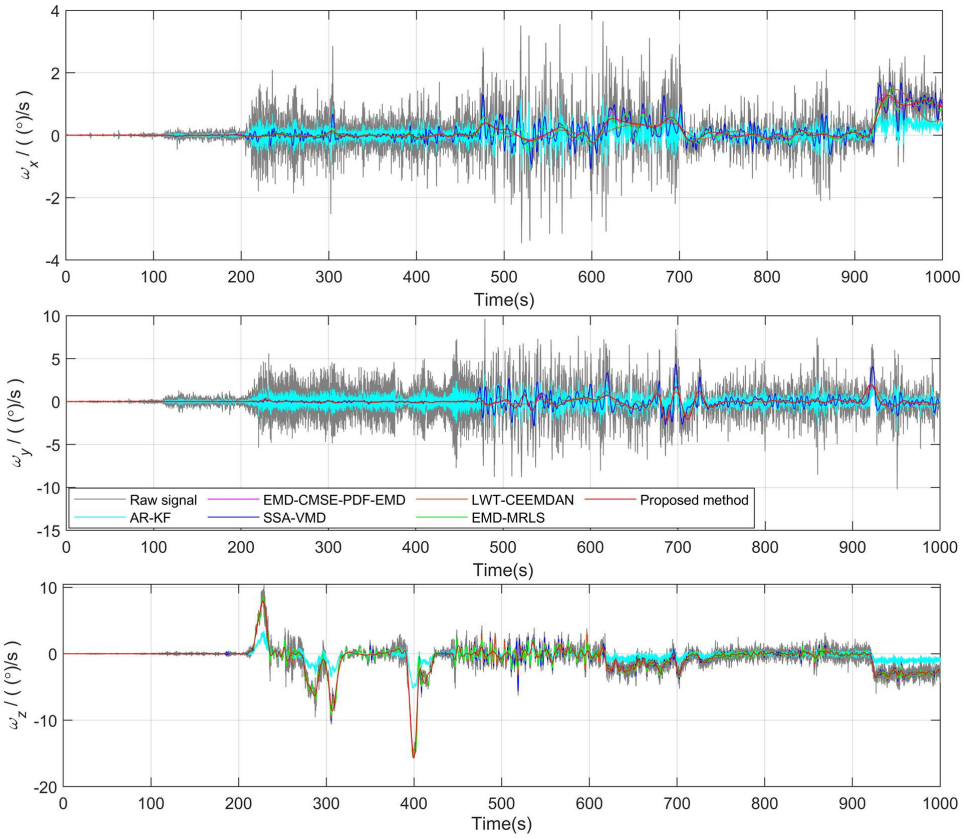

Fig. 11. Comparison of denoising results of the dynamic experiment.

In the figure, we find that the pitch and roll of the proposed method have a better convergence than other methods, but there is a slight deviation in the yaw, which indicates that the proposed method needs to be improved for the yaw.

In order to further verify the reliability of the scheme presented in this paper, the root mean square error of the three-axis attitude is calculated, as shown in Fig. 13.

As can be seen from the figure, in pitch and roll, the root-mean-square error of attitude is indeed the lowest of all methods, but in yaw, the root-mean-square error is slightly higher than that of Schemes 2 and 3. This verifies what has been mentioned above: in real-time applications, the proposed method has a good solution effect for pitch and roll, but for yaw, the effect is not as good as Schemes 2 and 3.

In order to verify the online applicability of the scheme presented in this paper, the calculation time of all schemes is given, as shown in Table 4. Compared with other methods, the time required by this method is slightly higher, which means that the calculation time required by this method is slightly higher than that of other methods for the same sampling time, but the calculation time of all methods is far lower than the sampling time, so this disadvantage has little impact on real-time performance. Meanwhile, from the point of view of the overall accuracy of the attitude, although the cost has been improved, the high precision of the attitude has made up for this shortcoming. In practical applications, this is undoubtedly a comparative advantage.

Metrol. Meas. Syst., Vol. 30 (2023), No. 4, pp. 755–772
DOI: 10.24425/mms.2023.147962

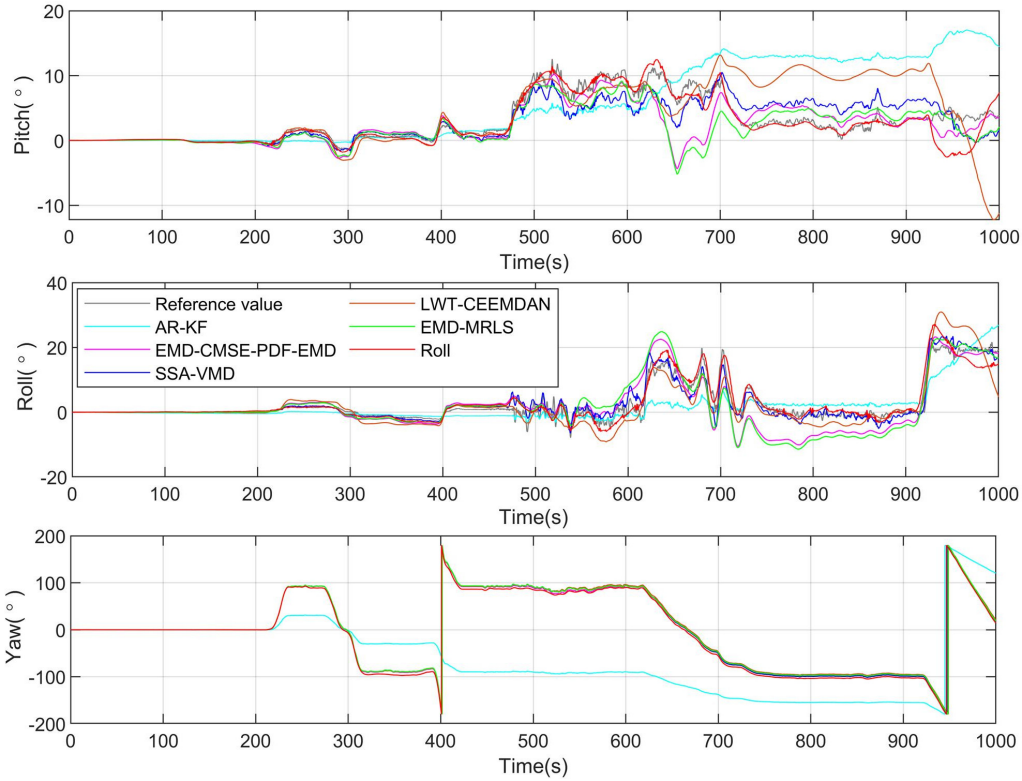

Fig. 12. Comparison of attitude approach results of the dynamic experiment.

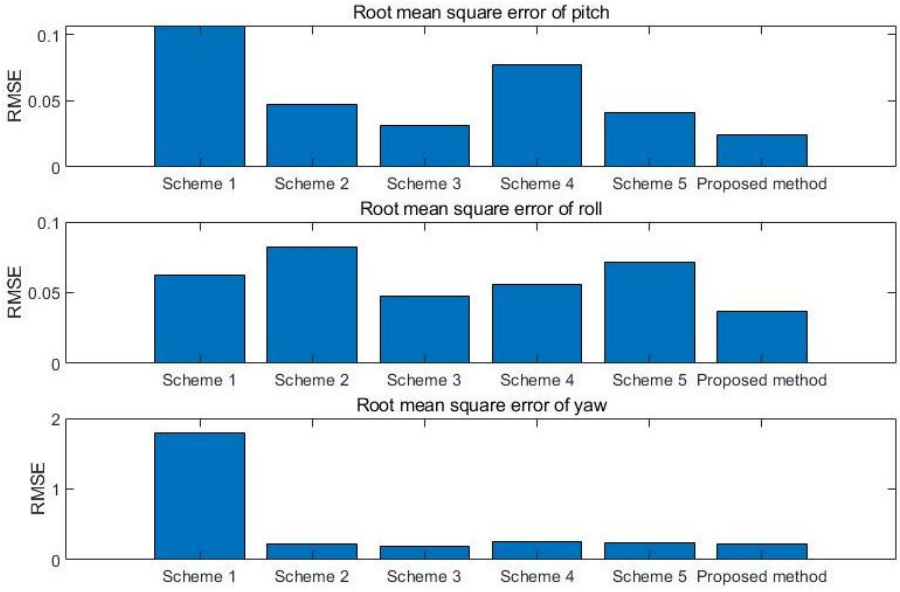

Fig. 13. Root mean square error of attitude estimates.

Table 4. Computation time for all schemes.

	Scheme 1	Scheme 2	Scheme 3	Scheme 4	Scheme 5	Proposed method
Time (s)	30.17	37.06	36.68	36.21	35.16	38.47

6. Conclusion

Based on the traditional EMD algorithm, this paper proposes a novel multiple screening mechanism which combines the Pearson coefficient, the entropy weight method and Shannon entropy. Unlike other optimized EMD methods that only divide IMFs into two or three categories, the proposed method divides IMFs into four categories after the first EMD decomposition. As the characteristics of the four types of IMFs are different, the least square algorithm and EMD were used for secondary processing. Thus, this method divides IMFs into two categories after the second EMD decomposition again. This method not only solves the difficulty of distinguishing IMFs, but also refines the denoising process, making the denoising result more effective. A MEMS gyroscope was used for experiment to verify the performance of the method. The experimental results show that the denoising effect of the proposed method is better than that of traditional denoising methods. Compared with methods proposed in recent years, the attitude accuracy of the inertial navigation solution is also significantly improved. It is concluded that this method has obvious effect for suppressing random error in gyroscope signals, and this method greatly improves signal quality and the accuracy of inertial navigation, so it has a certain guiding significance for engineering applications.

References

[1] Shen, C., Li, J., Zhang, X., Shi, Y., Tang, J., Cao, H., & Liu, J. (2016). A noise reduction method for Dual-Mass Micro-Electromechanical gyroscopes based on sample entropy empirical mode decomposition and Time-Frequency peak filtering. *Sensors*, *16*(5), 796. https://doi.org/10.3390/s16060796

[2] Hesham, M. A., Ibrahim, M. E., & Sami, A. E. (2022). Noise reduction in optical gyroscope signals based on hybrid approaches. *Journal of Optics*, *51*(1), 5–21. https://doi.org/10.1007/s12596-020-00617-3

[3] Xiaoting, G., Changku, S., Peng, W., & Lu, H. (2018). Hybrid methods for MEMS gyro signal noise reduction with fast convergence rate and small steady-state error. *Sensors and Actuators A: Physical*, *269*, 145–159. https://doi.org/10.1016/j.sna.2017.11.013

[4] Shuo, C., Yunfeng, H., Haitao, D., & Hong, C. (2018). A Noise reduction method for MEMS gyroscope based on direct modeling and Kalman filter. *IFAC-PapersOnLine*, *51*(31), 172–176. https://doi.org/10.1016/j.ifacol.2018.10.032

[5] Javad, A., Mojtaba, H., & Aria, A. (2022). A memory-based filter for long-term error denoising of MEMS-gyros. *IEEE Transactions on Instrumentation and Measurement*, *71*, 750–3308. https://doi.org/10.1109/TIM.2022.3178964

[6] Di, W., Xiaosu, X., Tao, Z., & Yongyun, Z. (2019). An EMD-MRLS de-noising method for fiber optic gyro Signal. *Optik*, *183*, 971–987. https://doi.org/10.1016/j.ijleo.2019.03.002

[7] Shuwen, D., & Lujun, L. (2020). Fiber optic gyro noise reduction based on hybrid CEEMDAN-LWT method. *Measurement*, *161*, 107–865. https://doi.org/10.1016/j.measurement.2020.107865

[8] Sun, T., & Liu, J. (2017). A novel noise reduction method for MEMS gyroscope. *Journal of Harbin Institute of Technology*, *49*(9), 0367–6234. https://doi.org/10.11918/j.issn.0367-6234.201606079

[9] Yingjie, H., & Lu, X. (2018). An integrated approach of wavelet techniques and time series analysis in eliminating MEMS inertial gyro stochastic error. *Automation and Systems*, *17*(20), 1834–5646. https://ieeexplore.ieee.org/document/8571935

[10] Zhang, N., & LiuYou, W. (2018). Signal de-noising model for MEMS gyro based on CEEMDAN improved threshold filtering. *Journal of Chinese Inertial Technology*, *26*(4), 1005–6734. https://doi.org/10.13695/j.cnki.12-1222/o3.2018.05.018

[11] Tao, L., Aigong, X., & Xin, S. (2018). EEMD interval threshold de-noising method for Inertial navigation. *Acta Geodaetica et Cartographica Sinica*, *7*, 907–915. https://doi.org/10.11947/j.AGCS.2018.20170391

[12] Lang, X., Desuo, C., Wei, S., & Huaizhi, S. (2021). Denoising method for fiber optic gyro measurement signal of face slab deflection of concrete face rockfill dam based on sparrow search algorithm and variational modal decomposition. *Sensors and Actuators A: Physical*, *331*, 112–913. https://doi.org/10.1016/j.sna.2021.112913

[13] Jian, L., Lixin, W., & Wenhua, L. (2022). MEMS gyro noise reduction method based on CEEMDAN multi-scale entropy. *Journal of Beijing University of Aeronautics and Astronautics*, 1001–5965. https://doi.org/10.13700/j.bh.1001-5965.2021.0745

[14] Bingbo, C., & Xiyuan, C. (2015). Improved hybrid filter for fiber optic gyroscope signal denoising based on EMD and forward linear prediction. *Sensors and Actuators A: Physical*, *230*, 150–155. https://doi.org/10.1016/j.sna.2015.04.021

[15] Mingkuan, D., Zhiyong, S., Binhan, D., Huaiguang, W., & Lanyi, H. (2021). A signal de-noising method for a MEMS gyroscope based on improved VMD-WTD. *Measurement Science and Technology*, *32*(8), 51–12. https://doi.org/10.1088/1361-6501/abfe33

[16] Santiago, G., & Alejandra, M. (2022). Indefinite least squares with a quadratic constraint. *Journal of Mathematical Analysis and Applications*, *514*(1), 126–297. https://doi.org/10.1016/j.jmaa.2022.126297

[17] Feng, D. (2023). Least squares parameter estimation and multi-innovation least squares methods for linear fitting problems from noisy data. *Journal of Computational and Applied Mathematics*, *426*, 115–107. https://doi.org/10.1016/j.cam.2023.115107

[18] Yaqing, L., & Yong, M. (2020). Daily activity feature selection in smart homes based on Pearson correlation coefficient. *Neural Processing Letters, 51*, 1771–1787. https://doi.org/10.1007/s11063-019-10185-8

[19] Degang, W., & Dongling, L. (2022). Fuzzy comprehensive evaluation of maritime boundary delimitation schemes based on AHP-entropy weight method. *Mathematical Problems in Engineering*, *13*, 275–7779. https://doi.org/10.1155/2022/2757779

[20] Kunshan, Y., & Jun, S. (2023). An information entropy-based grey wolf optimizer. *Soft Computing*, *27*, 4669–4684. https://doi.org/10.1007/s00500-022-07593-9

[21] Yan, G., Wang, J., & Zhou, X., High-precision simulator for strapdown inertial navigation systems based on real dynamics. *Journal of Navigation and Positioning*, *10*, 10–96. https://doi.org/10.16547/j.cnki.10-1096.20150406

[22] Yi, G., Donghang, L., & Piao, G. (2021). Aircraft attitude calculation based on gradient descent algorithm. *Electronic Design Engineering*, *23*, 0007–04. https://doi.org/10.14022/j.issn1674-6236.2021.23.002

Hailong Rong received the B.Sc. degree in automation and the M.Sc. degree in pattern recognition and intelligent systems from Northeastern University, Shenyang, China, in 2003 and 2006, respectively, and the Ph.D. degree in control theory and engineering from Southeast University, Nanjing, China, in 2010. He is currently with the School of Mechanical Engineering and Rail Transit, Changzhou University, Changzhou, China. His research interests are attitude tracking and pattern recognition based on magnetic and inertial measurement units.

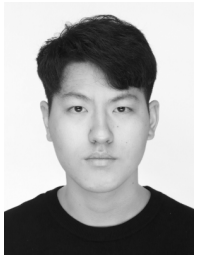

Tianlei Jin received his B.Sc. degree in electrical engineering automation from Linyi University in 2021. He is currently studying for a M.Sc. degree in mechanical engineering and rail transportation at Changzhou University, China. His main research interest is gyroscopic noise reduction.

Wang Hao obtained his B.Sc. degree in electrical engineering and automation from Changzhou University in 2021. He is currently pursuing a Master's degree in mechanical and electronic engineering from the School of intelligent manufacturing industry at Changzhou University. He mainly engages in research related to inertial sensors.

Xiaohui Wu received his B.Sc. degree in electrical engineering and automation from Anhui University of Technology in 2021. He is currently pursuing his M.Sc. at the School of Mechanical Engineering and Railway Transportation at Changzhou University, China. His research interests are deep learning-based IMU attitude estimation.

Ling Zou received her Ph.D. degree in control science and control engineering from Zhejiang University, Hangzhou, China, in 2004. She is currently a professor with the School of Microelectronics and Control Engineering, Changzhou University, Changzhou, China. Her research interests are control engineering, biomedical signal processing, and pattern recognition.